THE ROLE OF CLAY MINERALS IN THE PRESERVATION OF ORGANIC MATTER IN SEDIMENTS OF QINGHAI LAKE, NW CHINA

Bingsong Yu[1], Hailiang Dong[1,2,*], Hongchen Jiang[2], Guo Lv[1], Dennis Eberl[3], Shanying Li[1], and Jinwook Kim[4]

[1] Geomicrobiology Laboratory, State Key Laboratory of Geological Processes and Mineral Resources, China University of Geosciences, Beijing, China, 100083
[2] Department of Geology, Miami University, Oxford, OH 45056, USA
[3] US Geological Survey, Boulder, CO 80303, USA
[4] Department of Earth System Sciences, Yonsei University, Seoul, Korea

Abstract—The role of saline lake sediments in preserving organic matter has long been recognized. In order to further understand the preservation mechanisms, the role of clay minerals was studied. Three sediment cores, 25, 57, and 500 cm long, were collected from Qinghai Lake, NW China, and dissected into multiple subsamples. Multiple techniques were employed, including density fractionation, X-ray diffraction, scanning and transmission electron microscopy (SEM and TEM), total organic carbon (TOC) and carbon compound analyses, and surface area determination. The sediments were oxic near the water-sediment interface, but became anoxic at depth. The clay mineral content was as much as 36.8%, consisting mostly of illite, chlorite, and halloysite. The TEM observations revealed that organic matter occurred primarily as organic matter-clay mineral aggregates. The TOC and clay mineral abundances are greatest in the mid-density fraction, with a positive correlation between the TOC and mineral surface area. The TOC of the bulk sediments ranges from 1 to 3% with the non-hydrocarbon fraction being predominant, followed by bitumen, saturated hydrocarbon, aromatic hydrocarbons, and chloroform-soluble bitumen. The bimodal distribution of carbon compounds of the saturated hydrocarbon fraction suggests that organic matter in the sediments was derived from two sources: terrestrial plants and microorganisms/algae. Depth-related systematic changes in the distribution patterns of the carbon compounds suggest that the oxidizing conditions and microbial abundance near the water-sediment interface promote degradation of labile organic matter, probably in adsorbed form. The reducing conditions and small microbial biomass deeper in the sediments favor preservation of organic matter, because of the less labile nature of organic matter, probably occurring within clay mineral-organic matter aggregates that are inaccessible to microorganisms. These results have important implications for our understanding of mechanisms of organic matter preservation in saline lake sediments.

Key Words—Carbon Compounds, Clay Minerals, Organic Matter, Preservation, Qinghai Lake, SEM, TEM, XRD.

INTRODUCTION

Saline-lake deposits of Cenozoic age are among the most important petroleum source rocks in China (Sun *et al*., 1997). Saline lakes possess several characteristics that are favorable to the formation of hydrocarbons. Among these are high primary productivity, favorable enrichment and preservation conditions, abundant organic matter, and a high conversion rate of organic matter to hydrocarbons (Sun *et al*., 1997). Based on a systematic study of enrichment and preservation of organic matter in evaporite deposits, their temporal-spatial distribution patterns, and biomarkers, Li (1993) emphasized the potential of petroleum generation in hypersaline sedimentary environments. Despite the importance of saline lakes, the occurrence of organic matter in saline-lake sediments and their preservation mechanisms are still poorly understood.

Most published studies on preservation mechanisms of organic matter are focused on marine sediments, where organic matter is largely associated with clay minerals (Keil and Hedges, 1993; Mayer 1994a; Hedges and Keil, 1995, 1999; Hedges and Oades, 1997; Bock and Mayer, 2000; Arnarson and Keil, 2001). The organic matter-clay mineral association has been recognized for several decades, *e.g.* Bader *et al*. (1970) reported that clay minerals play an important role in sorbing organic matter. However, the mechanisms of clay mineral-organic matter interactions and the quantitative relationship between organic matter in sediments and mineral surface area (MSA) were not fully investigated until relatively recently (Keil and Hedges, 1993; Mayer, 1994a, 1994b; Hedges and Keil, 1995, 1999; Hedges and Oades, 1997).

In the last decade, important advances have been made regarding the mechanisms and extents of clay

mineral-organic matter associations. One important observation is the strong positive correlation between TOC content of continental margin sediments and MSA (Mayer, 1994b; Mayer, 1999; Ransom *et al.*, 1998; Bergamashi *et al.*, 1997; Bock and Mayer; 2000), suggesting that TOC may be sorbed onto clay mineral surfaces. Indeed, transmission electron microscope (TEM) observations revealed that organic carbon occurs as irregular coatings on mineral surfaces (Ransom *et al.*, 1998; Bishop *et al.*, 1992; Ransom *et al.*, 1997), especially on clay mineral surfaces, with <10% as discrete particulates. Once desorbed from mineral surfaces, organic matter may be quickly degraded by microbial activity (Keil and Hedges, 1993; Bergamashi *et al.*, 1997). Adsorbed, degradable organic matter may be protected from microbial activity through its physical isolation from the outside world (Bader *et al.*, 1970; Gordon and Millero, 1985; Heinrichs and Sugai, 1993; Bishop and Phillip, 1994; Collins *et al.*, 1995; Salmon *et al.*, 2000; Keil and Hedges, 1993; Mayer, 1994a; Hedges and Keil, 1995). Curry *et al.* (2007) studied polysaccharides, an abundant class of organic matter in marine sediments, associated with the nano- and microfabrics of clay-rich sediments. Those authors employed multiple techniques and concluded that organic matter sorbed onto clay surfaces and/or encapsulated within clay microfabrics was protected from microbial degradation.

The close association between clay minerals and organic matter is further revealed by the observation that organic matter is mainly concentrated in mid-density sediments (1.6−2.2 g/cm^3), where fine-grained clay minerals are also concentrated. A recent study showed that the mid-density fraction of organic-rich marine sediments consisted of 62% and 80% of the sedimentary mass (largely clay mineral smectite) and organic matter, respectively (Arnarson and Keil, 2001). In these marine sediments, organic matter did not occur as simple adsorbents uniformly distributed on clay mineral surfaces (Bock and Mayer, 2000; Arnarson and Keil, 2001).

Qinghai Lake is the largest inland saline lake in China. In the lake sediments, the TOC content reaches 3% and clay minerals are abundant. The objective of this study was to investigate the relationship between organic matter and clay minerals and to provide mineralogical and sedimentary constraints on the preservation of organic matter. Although the Qinghai lake sediments do not have a large TOC content, they do possess certain characteristics that warrant further study, *e.g.* organic matter in Qinghai lake sediments has undergone burial and transition to hydrocarbons (Sciences, 1979). The lake harbors certain microorganisms that are common in organic-rich marine sediments (Dong *et al.*, 2006; Jiang *et al.*, 2008). In the present study, a suite of analytical techniques, including density fractionation, quantitative X-ray diffraction (XRD), TOC content and organic compound analyses, mineral surface area (MSA), and SEM and TEM, was employed. The results indicate that

organic matter in Qinghai Lake sediments occurs as clay mineral-organic matter aggregates which may favor the preservation of organic matter in lake sediments.

MATERIALS AND METHODS

Study site and sampling

Qinghai Lake is a perennial lake located in a structural intermontane depression at the northeastern corner of the Qinghai-Tibetan Plateau (Figure 1). The lake is 4300 km^2 in area and lies within a catchment of limestones, sandstones, and shales (Henderson *et al.*, 2003). The average water depth is 19.2 m, and the maximum is 28.7 m. The altitude of the lake is 3196 m above sea level (m.a.s.l.), and the surrounding mountains rise to >5200 m.a.s.l. (Dong *et al.*, 2006). The evaporation of the lake (~1400 mm/y) is in excess of mean annual precipitation (~400 mm/y), resulting in the development of a saline lake with salinity of 12.5 p.s.u. (practical salinity units) (Dong *et al.*, 2006; Shen *et al.*, 2005).

A recent seismic survey suggests that Qinghai Lake is separated into two sub-basins by a normal faulting horst in the middle of the lake (An, 2003). The northern sub-basin is more dynamic than the southern one because of a major river input in the northwest and a strong prevailing northwest wind. The entire water column in the northern sub-basin is well mixed in summer. In comparison, the southern sub-basin is relatively quiet; the depositional environment is stable, and water stratification occurs seasonally (Sciences, 1979). Dissolved oxygen typically shows a slight gradient from 6 ppm at the surface to 3 ppm at the bottom of the water column in the eastern depression of the southern sub-basin (~23 m water depth) (Dong *et al.*, 2006), within which the sampling sites were selected ~20 km north of a fishing station, called Erlangjian, for easy access (E: 100º34′16.9′′, N: 36º36′35.3′′) (Figure 1) and stable depositional environment. The water depth at the sampling site was 25 m.

Three cores were collected from adjacent sites (Figure 1). The two short cores were collected using a gravity-driven coring device. The first short core was 25 cm long, the second, 57 cm long. The first core was dissected into 5 cm long subsamples (from the bottom to the top: QH1-1 to QH1-5). The second core was dissected into 9 cm subsamples with the top sample being 12 cm long (from the bottom to the top: QH2-1 to QH2-6). The third core was 5 m long and collected using a drilling platform. It was dissected into 15 cm subsamples (QH3-1 to QH3-33). Visual inspection revealed that the top of each core (at the water-sediment interface) was reddish-brown in color, suggesting oxidizing conditions, whereas the deeper sediments were black in color, suggesting reducing conditions. Hydrogen sulfide odor was also evident from the deeper portions of the cores.
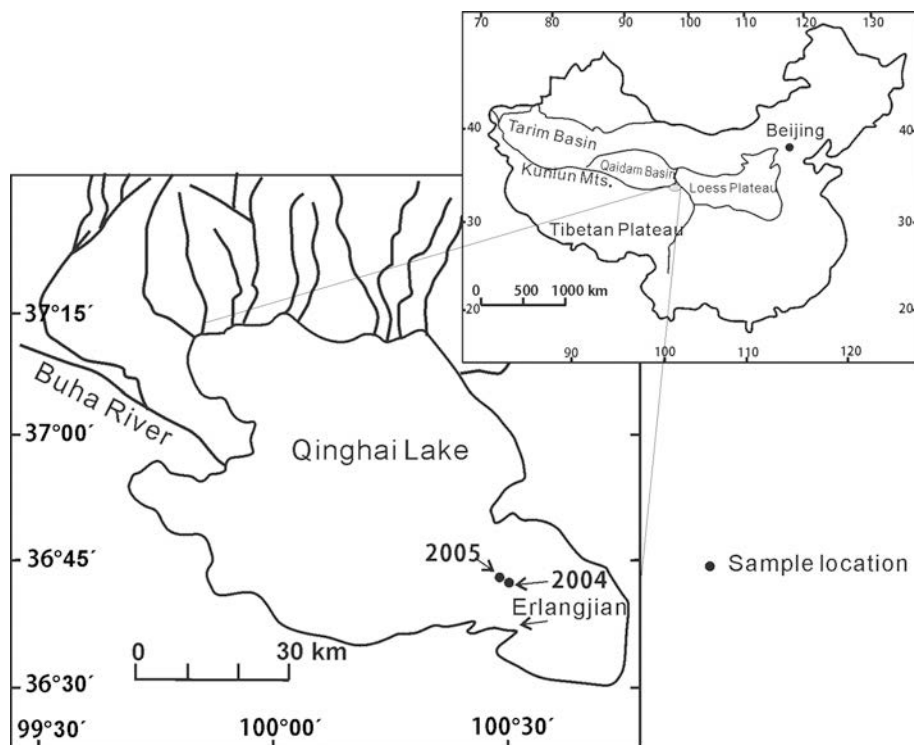
Figure 1. Location map of Qinghai Lake showing the drilling sites of the three cores used in this study.

Density fractionation

Because of the lower density of organic matter than clay minerals, organic matter-clay mineral aggregates should be less dense than clay minerals. Thus, density-based clay-mineral fractionation is commonly used to separate organic matter-clay mineral aggregates from pure clay minerals and to study the relationship between organic matter and minerals (Turchenek and Oades, 1976; Golchin *et al.*, 1994; Hedges and Oades, 1997; Bock and Mayer, 2000; Arnason and Keil, 2001). A previous study showed that the density cut-off value between minerals and organic matter in marine sediments is 1.9 g/cm^3 (Mayer, 1994a), a value used initially in the present study to separate organic materials from mineral phases. Organic matter-clay mineral aggregates should have higher density, however, with specific values depending on the clay mineralogy and the nature of the organic materials. The XRD results (see below) showed that illite and chlorite were the dominant clay minerals. Given the density of illite and chlorite (2.5−2.8 and 2.7−3.4 g/cm^3, respectively), their respective surface areas (65−100 m^2/g) (Zhao and Zhang, 1990), a previously published value of sorption capacity of organic carbon on clay minerals (1 mg/m^2) (Mayer, 1994a, 1994b), and density of organic carbon (~1 g/cm^3), the present authors estimated that the density of organic matter-clay mineral aggregates should be <2.8 g/cm^3. Therefore, the subsamples from the first

core (QH1-1 through QH1-5) were separated into three fractions, *i.e.* <1.9 g/cm^3, 1.9−2.8 g/cm^3, and >2.8 g/cm^3 using sodium polytungstate (3Na$_2$WO$_4$.9WO$_3$.H$_2$O, maximum density, 3.1 g/cm^3) as a heavy liquid (Sometu, Germany). This heavy liquid has been used for density fractionation by previous workers and has a number of advantages over other chemicals. The highly soluble inorganic salt, sodium polytungstate, when dissolved in water, can be used to replace the toxic and possibly carcinogenic organic liquids traditionally used for gravity separation work. This liquid has a low viscosity even at high concentrations and is stable over the pH range of 2−14. This compound does not destroy any organic matter (Bock and Mayer, 2000) and can be made to have a wide range of densities, up to 3.1 g/cm^3.

The subsamples from the first core (QH1-1 through QH1-5) were air dried and ground with a mortar and pestle. The low-density fraction was separated first by mixing a known amount of sediment with sodium polytungstate (with a final density of 1.9 g/cm^3) followed by centrifugation at 4000 g for 100 min. Any particles with density <1.9 g/cm^3 were in suspension and subsequently collected by filtration. The pellets at the bottom of the centrifuge tube were re-mixed with sodium polytungstate (with a final density of 2.8 g/cm^3). Following centrifugation, the mid- and high-density fractions were collected in a similar fashion. The density-fractionated sediment fractions were washed

thoroughly with distilled water to remove any residual sodium polytungstate.

Quantitative mineralogical analysis by X-ray diffraction

X-ray diffraction (XRD) was performed to identify mineral phases in the bulk sediments and the density-fractionated fractions. Quantitative mineralogical analysis of the bulk lake sediments was performed at the United States Geological Survey (USGS) using the *RockJock* program which calculates the proportion of a mineral in a complex mixture by comparing the integrated intensity of a characteristic diffraction peak of that mineral to the intensity of the same peak of an internal standard (Środoń *et al.*, 2001; Eberl, 2003). Samples were X-rayed with a Siemens D500 X-ray diffraction system using CuKα radiation, 40 kV, 100 mA current, a monochromator, and were scanned in $0.02°2\theta$ steps from 5 to $65°2\theta$.

The density-fractionated fractions were analyzed at the X-ray diffraction laboratory of China Petroleum Exploration and Development Research Center in Beijing. Previous SEM observations indicated that clay minerals were concentrated in the mid-density fraction, and the low- and high-density fractions were largely composed of organic materials (such as pollen and plant residuals) and detrital minerals, respectively. Therefore, XRD analysis was performed on the mid-density fraction only ($1.9-2.8$ g/cm^3). The samples were dispersed in 1 mL of distilled water using an ultrasonic probe. An oriented sediment film was prepared by repeated pipetting and settling of sediment slurry onto a glass slide followed by air-drying. All the samples were prepared with the same method and had approximately the same thickness. The samples were X-rayed with a D/max 2500 X-ray diffraction system using CuKα radiation, 40 kV, 100 mA current, a monochromator, and were scanned in $0.02°2\theta$ steps from 2.6 to $30°2\theta$, with a count time of 2 s per step. In order to identify the possible presence of smectite-illite mixed layers, the glass slides containing oriented sediment powder of the mid-density fractions were treated with ethylene glycol for 7.5 h at 60ºC. The positions of the peak maxima were compared with those calculated by the NEWMOD program (Christidis and Eberl, 2003).

Total organic carbon (TOC) analysis

For the first core, both the density-fractionated and bulk sediments were used for TOC analyses. For selected subsamples from the second and the third cores, only the bulk sediments were analyzed. For the samples from the first and second cores, the TOC content was determined using a LECO-CS400 CS analyzer following removal of inorganic carbon (by reacting with 0.1 N HCl) for 2 h at 60−80ºC. The TOC was combusted into CO_2 which was quantified with an infrared detector. For the bulk-sediment subsamples from the third core, the TOC content was determined using a Perkin-Elmer 2400 CHNS analyzer at Miami University, Oxford, Ohio, USA.

Organic component/compound analysis

The subsamples from the second core were selected for organic-component analysis. The chloroform-soluble bitumen 'A' and other organic components (saturated hydrocarbons, aromatic hydrocarbons, non-hydrocarbons, and bitumen) were determined by a Thin Layer IATROSCAN MK-5 chromatography system at a temperature of 22ºC and a relative humidity of 25%. The TOC in the sediments was dissolved with chloroform to a final concentration of 10−20 mg/mL. Approximately 0.5−1.0 µL of this solution was extracted with a micro-injector and added to an activated silica gel chromatographic column. Different components of the extracted organic matter were separated chromatographically using n-hexane, n-hexane-methylene chloride (1:1), and hexylene:isoamyl alcohol (90:10). The components were analyzed with a thin-layer chromatography/flame ionization analyzer. Peak area, after background subtraction, was used to calculate the mass fraction of each component.

The saturated hydrocarbon component was further analyzed for carbon compounds with an HP-5890 gas chromatograph with an OV-1 elastic silica capillary column (25 m × 0.22 mm i.d.). Samples of saturated hydrocarbon were injected into a vaporization chamber. Following vaporization, all carbon compounds, together with the carrier gas, were introduced into the capillary column. After separation, each compound was detected with a flame ionization detector. Background-subtracted peak area was used to determine the relative mass fraction of each compound.

Mineral-surface-area analysis

The BET surface areas of selected density-fractionated fractions and bulk sediment subsamples of the three cores were measured using a Coulter SA3100 analyzer, which utilizes an adsorbed volume of liquid nitrogen to calculate the surface area.

SEM and TEM

Following XRD, the sediment mineralogy was further studied using SEM and TEM. Sediments were sprayed onto SEM stubs (with sticky carbon tape on the surface) and Au coated for observation using a Zeiss, low-vacuum SEM. The SEM was operated at an accelerating voltage of 10 to 15 kV. A short working distance (6−10 mm) and small probe current (30−40 mA) were used to achieve the best image resolution. A longer working distance (8.0 mm) and greater probe current (50−70 mA) were used for qualitative energy dispersive spectroscopy (EDS) analysis.

To observe the spatial relationship between organic matter and clay minerals, the mid-density fraction of the deepest subsample of the first core (QH1-5) was selected

Table 1. Relative proportions of the low-, mid-, and high-density fractions of the Qinghai Lake sediments.

Sample no.	QH1-1		QH1-2		QH1-3		QH1-4		QH1-5	
	Wt.(g)	Wt.%	Wt.(g)	Wt.%	Wt.(g)	Wt.%	Wt.(g)	Wt.%	Wt.(g)	Wt.%
Original	47.3		61.1		60.5		53.1		49.1	
Low-density	0.1	0.2	0.1	0.2	0.1	0.2	0.1	0.3	0.2	0.3
Mid-density	11.4	24.2	5.0	8.1	2.5	4.2	1.0	2.0	1.9	3.8
High-density	33.1	70.0	52.5	85.9	55.9	92.4	50.1	94.3	47.3	96.4
Recovery (%)		94.4		94.2		96.8		96.6		100.4

for high-resolution TEM observations, selected area electron diffraction (SAED), and energy dispersive spectroscopy (EDS). Unconsolidated sediments were dispersed in ethanol and the sediment slurry was mounted onto formvar-coated copper grids and observed using a JEOL 3010 TEM operating at 300 keV with a LaB_6 filament. Images were taken at various magnifications.

RESULTS

Density fractionation

The recovery of density-fractionated sediments was >94% with an average of 96.5%, indicating little loss or gain during the fractionation. The results revealed that the Qinghai lake sediments are dominated by the high-density fraction (70.0−96.4%, Table 1). The low-density and mid-density fractions comprised 0.2−0.3% and 2.0−24.0% of the lake sediments, respectively.

XRD, SEM, and TEM characterization of the sediments

Quantitative XRD results indicate that the bulk sediments (of the first core) consist of non-clay minerals (54%) and clay minerals (37%). The non-clay minerals include aragonite (16%), quartz (14%), plagioclase (9%), K-feldspar (3), calcite (9%), dolomite (2%), and amphiboles (1%) in decreasing order of abundance. The clay minerals include illite of $1M_d$, $1M$, and $2M_1$ polytypes (24%), chlorite (10%), and halloysite (3%).

The XRD patterns for the density-fractionated sediments indicate that the clay minerals are concentrated in the mid-density fraction (Table 2), reaching as much as

65% in QH1-5. Illite is the predominant clay mineral with some mixed-layer illite-smectite (I-S). The proportion of smectite in mixed-layer I-S is usually <15%, suggesting that the mixed-layer I-S is highly illitic. The XRD patterns show a hump-shaped background for the high-TOC samples (Figure 2), suggesting that TOC is largely amorphous. In comparison, those XRD patterns for the low-TOC samples show a smaller background.

Observations by SEM and EDS analyses confirm the presence of the major minerals in the bulk sediments (Figure 3a,b). Carbonates occur as euhedral crystals. Illite occurs in two different morphologies: large flakes and small, fluffy-looking aggregates. These two forms may correspond to $2M_1$ mica and $1M_d$ ($1M$) illite, respectively, as identified by XRD. Pollen and plant debris dominate the low-density fraction (Figure 3c), whereas clay minerals are abundant in the mid-density fraction, and quartz, feldspars, and calcite are predominant in the high-density fraction (data not shown). Framboidal pyrite is also observed under SEM.

The TEM observations show that organic matter occurs in association with clay minerals (Figure 3d). Illite is the dominant clay mineral and was identified based on EDS analyses and SAED patterns (data not shown). The SAED pattern revealed that the organic matter is largely amorphous (Figure 3e). The EDS analysis identified minor amounts of certain metals associated with organic matter, including Ca, Cr, Fe, and Co (Figure 2f). Some of these metals may be from impurities of residual sodium polytungstate, the heavy liquid used in the density separation, as observed in a

Table 2. Results of quantitative mineralogical analysis by XRD for the mid-density fractions ($1.9 < \rho \leqslant 2.8/cm^3$) of the sediments from Qinghai Lake

Density fraction	Non-clay minerals (%)				Clay minerals (%)				
	Q	F	C	A	I-S	I	K	Ch	S/I (%S)
QH1-1	7	3	9	47	8	19	2	4	15
QH1-2	42	16	8	n.d.	12	15	2	4	10
QH1-3	32	18	5	n.d.	9	28	4	5	10
QH1-4	33	13	8	n.d.	10	28	3	5	10
QH1-5	20	5	9	n.d.	23	30	5	7	10
Average	27	11	8	n.d.	12	24	3	5	11

Q: quartz; F: feldspars; C: calcite; A: aragonite; n.d.: not detected.
I-S: illite-smectite mixed-layer phases; I: illite, K: halloysite; Ch: chlorite; S/I: the percent of smectite layers within I-S.
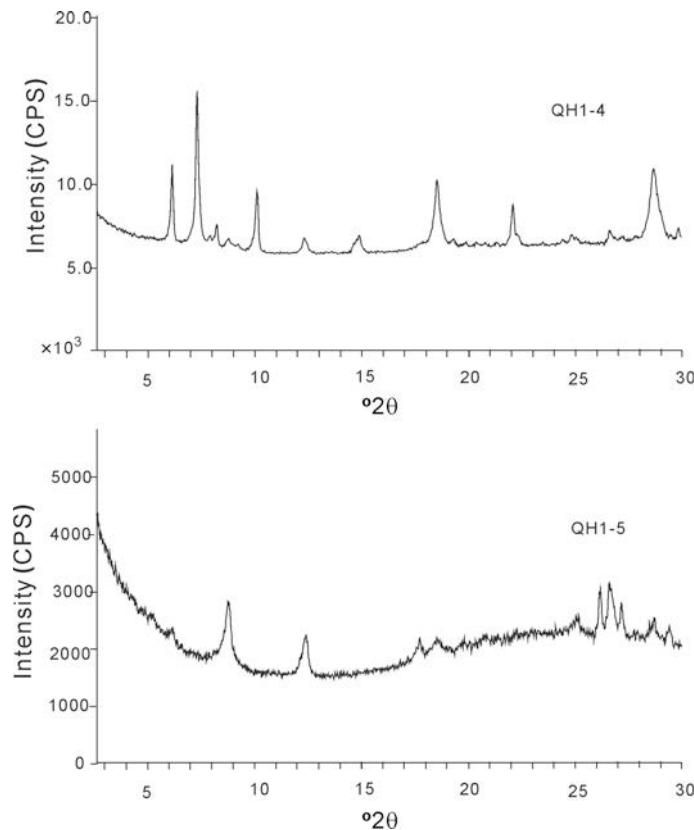
Figure 2. Two representative XRD patterns of the mid-density fractions of core QH1 (QH1-5 and QH1-4) showing the difference in the background. The high-TOC sample (QH1-5) shows a characteristic hump-shaped background confirming the large TOC (2.89%). In comparison, the low-TOC sample (QH1-4, 1.08% TOC) did not show this hump.

previous study (Arnarson and Keil, 2001). The associations of metals with organic matter in sediments and sedimentary rocks are also commonly observed, however (Peacor *et al*., 2000).

TOC and surface area

The TOC content of the bulk sediment samples ranges from 1 to 3% with an average of 2% (Table 3, Figure 4). Relative to the bulk sediment, the TOC is concentrated in the mid-density fraction (2.01 *vs*. 2.83 for QH1-1). Likewise, the MSA of the mid-density fraction was the greatest among all three fractions ranging from 6.7 to 19.9 m^2/g. The positive correlation between TOC and MSA suggests that the TOC was associated with the clay minerals (Figure 4), confirming the TEM observations (Figure 3d).

Depth-profile of organic matter components in relation to biomass distribution

Component-specific analyses indicated that the non-hydrocarbon component is predominant (Table 4), ranging from 68.65 to 78.95% with an average of 74.94%. The bitumen fraction ranges from 16.82 to 26.12% with an average of 21.35%, the saturated hydrocarbons from 1.61 to 6.24% with an average of 3.45%, the aromatic

hydrocarbons from 0.13 to 0.64% with an average of 0.26%, and the chloroform-soluble bitumen 'A' fraction from 0.04 to 0.1% with an average of 0.06%. Because saturated hydrocarbons, aromatic hydrocarbons, and bitumen are degradation products of organic matter, the sum of these three components, after normalization to TOC, represents the extent of bulk organic-matter degradation. When the extent of this degradation was plotted parallel to the depth profile of total biomass, as determined by acridine orange direct count (AODC) (Dong *et al*., 2006), a corresponding pattern was revealed. The greatest extent of degradation (Figure 5a) at the top of the core corresponded to the greatest abundance of total biomass (Figure 5b). With increasing depth in the sediments, both the extent of degradation and biomass decreased.

Carbon compounds of the saturated hydrocarbon component

The results of carbon compounds of the saturated hydrocarbon fraction revealed a bimodal distribution pattern with C_{max} at C17 and C29, respectively (Figure 6). The odd-even predominance (OEP) is obvious for the main peak (high-carbon peak), but not present for the secondary peak (low-carbon peak). The
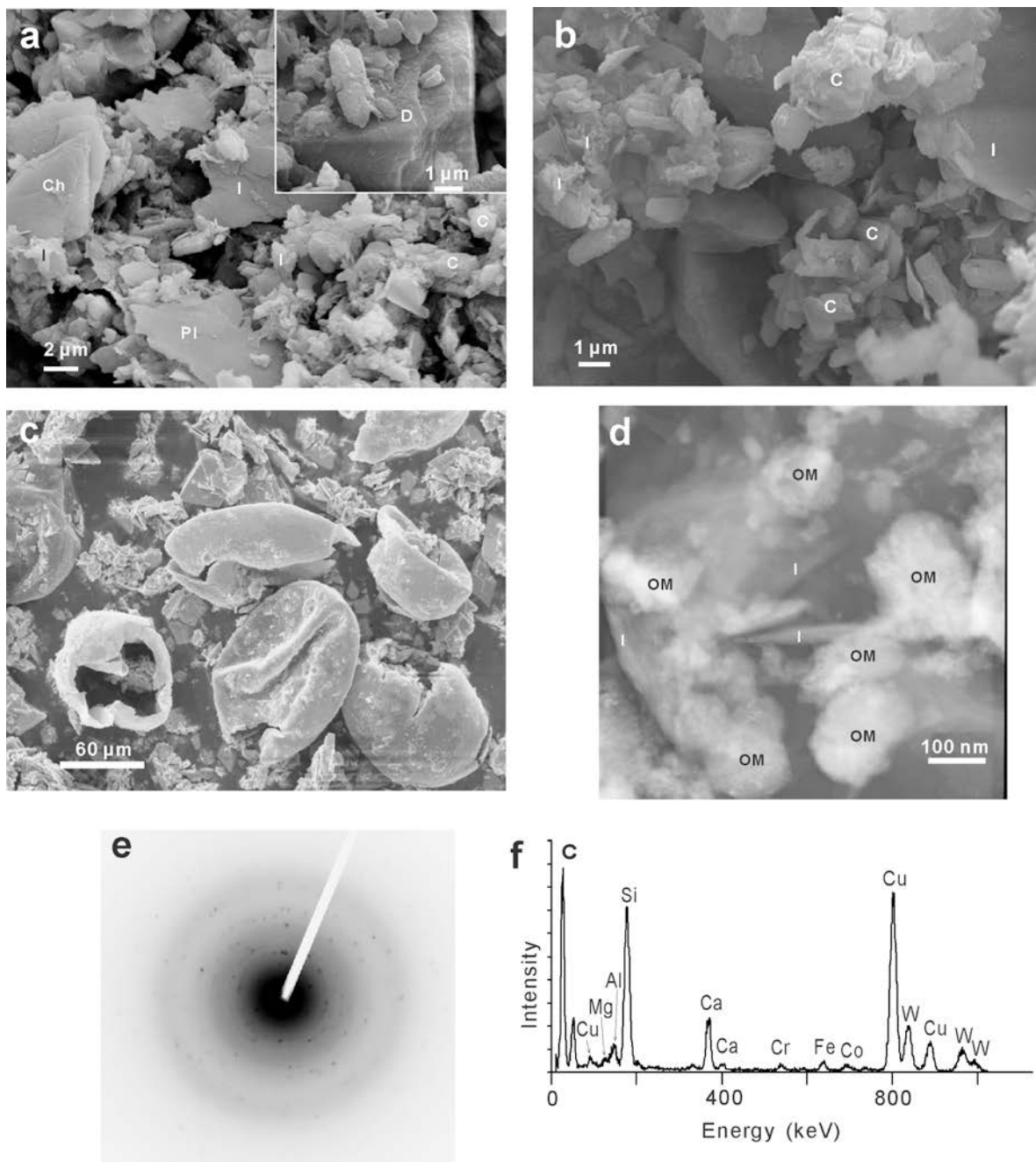
Figure 3. SEM and TEM images showing various minerals and organic matter in the Qinghai Lake sediments. (a,b) SEM images showing the dominant minerals: D − dolomite; I − illite; C − calcite; Ch − chlorite; Pl − plagioclase; (c) SEM image showing pollens in the low-density faction; (d) TEM image showing the association between the organic matter and the clay minerals. Organic matter (OM) occurs among clay mineral (I) packets as organic matter-clay minerals aggregates; (e) Selected area electron diffraction (SAED) pattern showing the amorphous nature of the organic matter; (f) EDS spectrum of organic matter showing that certain metals were associated with the organic matter including Ca, Cr, Fe, and Co. The Cu peaks are from the TEM Cu grid.

distribution pattern varies systematically with sediment depth. With increasing depth, the relative abundance of the low-carbon peak (consisting of those compounds with carbon number $\leqslant 22$) increases, whereas the relative abundance of the high-carbon peak (consisting of those compounds with the carbon number $\geqslant 23$) decreases. The C_{max} of the low-carbon peak shifted from 17 to 16 with increased depth (Figure 5), however, the C_{max} of the high-carbon peak remained at the same position (C29).

Table 3. TOC contents and mineral surface areas of Qinghai Lake sediments.

Sample no.	Depth (cm)	Density (g/cm^3)		TOC (%)	Mineral surface area (MSA) (m^2/g)	TOC/MSA (mg/m^2)
QH1-1	20−25	$1.9<\rho\leqslant2.3$	2.83	2.01	19.9	1.4
		$2.3<\rho\leqslant2.8$	1.52		−	−
		$\rho>2.8$	1.96		−	−
QH1-2	15−20	$1.9<\rho\leqslant2.8$	1.31	1.12	6.7	2.0
		$\rho>2.8$	1.11		5.6	1.4
QH1-3	10−15	$1.9<\rho\leqslant2.8$	1.44	0.93	10.3	2.0
		$\rho>2.8$	0.91		6.3	1.5
QH1-4	5−10	$1.9<\rho\leqslant2.8$	1.08	0.99	−	−
		$\rho>2.8$	0.99		−	−
QH1-5	0−5	$1.9<\rho\leqslant2.8$	2.89	1.19	−	−
		$\rho>2.8$	1.13		6.1	1.9
QH1-2	15−20	Bulk		1.12	1.8	6.2
QH1-5	0−5	Bulk		1.19	7.0	1.7
QH3-1	1−10	Bulk		3.04	7.83	3.9
QH3-2	13−26	Bulk		2.07	6.80	3.0
QH3-4	45−59	Bulk		2.79	8.58	3.2
QH3-6	74−89	Bulk		2.22	10.93	2.0
QH3-14	209−224	Bulk		2.48	10.73	2.3
QH3-19	286−300	Bulk		2.38	9.60	2.5
QH3-21	317−328	Bulk		2.55	7.01	3.6
QH3-23	338−345	Bulk		2.44	7.75	3.1
QH3-25	375−389	Bulk		2.94	13.47	2.2
QH3-27	399−415	Bulk		1.65	10.49	1.6

TOC: total organic carbon; −: no measurements; MSA: mineral surface area.

In addition to the depth-related changes in the relative abundance of the two peaks, a number of geochemical parameters also showed systematic trends. The ratio of pristane to phytane (Pr/Ph), indicative of the redox potential of the source sediments (Didyk *et al*., 1987; Hughes *et al*., 1995), showed a decreasing trend with increased depth (Figure 7a), consistent with the visual inspection of the color change of the core, *i.e.* oxidizing conditions near the top of the water-sediment interface to reducing conditions deeper in the sediments. The Pr/Ph ratios of slightly >1 for the lower portion of the core, which is under reducing conditions, may be due to the fact
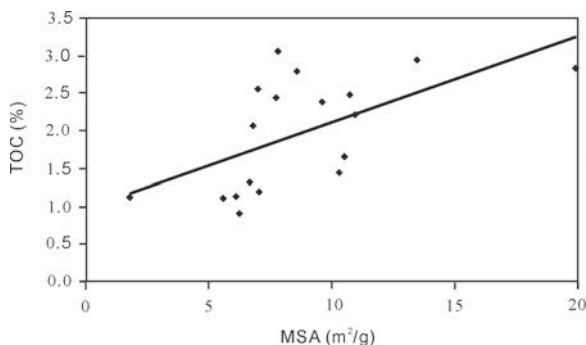
Figure 4. Positive correlation between TOC and MSA in the Qinghai Lake sediments.
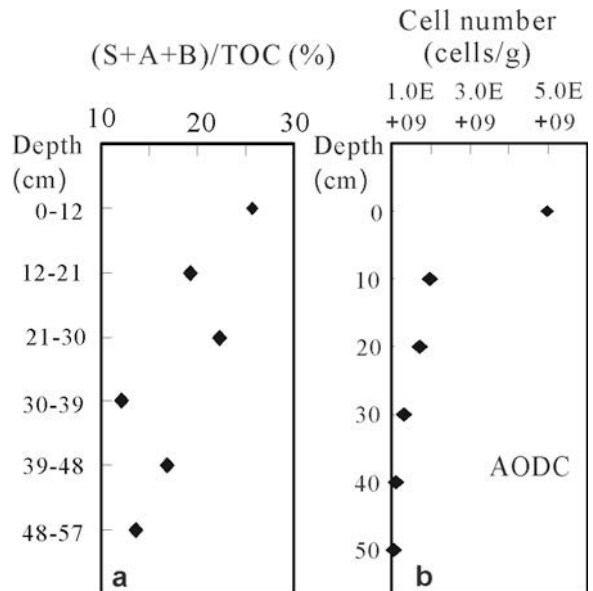
Figure 5. (a) The extent of bulk organic matter degradation (plotted as the sum of the saturated hydrocarbon (S), aromatic hydrocarbon (A), and bitumen fractions (B) relative to TOC) with depth; (a) Depth profile of total biomass (the data are from Dong *et al*., 2006)

Table 4. TOC and its components in Qinghai Lake sediments (%).

| Sample No.	TOC	'A'	S	A	N	B
QH2-6	1.22	0.04	2.78	0.13	68.65	28.44
QH2-5	1.26	0.05	6.24	0.64	75.71	17.41
QH2-4	1.35	0.04	3.85	0.19	69.83	26.12
QH2-3	1.73	0.07	1.61	0.17	78.95	19.27
QH2-2	1.28	0.05	4.44	0.29	78.45	16.82
QH2-1	1.61	0.11	1.80	0.15	78.02	20.03
Average	1.41	0.06	3.45	0.26	74.94	21.35

TOC: total organic carbon; 'A': chloroform-soluble bitumen; S: saturated hydrocarbons; A: aromatic hydrocarbons; N: non-hydrocarbons; B: bitumen.

that the sediments have not had sufficient time to reach equilibrium with the overall reducing condition. The ratios of pristane to C17 and phytane to C18, indicative of organic-matter maturity (Wang, 1990), showed a similar trend of decrease with increased depth (Figure 7b,c), suggesting increased organic-matter maturity at depth. The abundance ratio of all compounds with C<21 to all compounds with C>22, indicative of organic matter source and maturity (Wang, 1990), increaseed with depth (Figure 7d). In summary, these depth profiles of

Table 5. Carbon compounds of saturated hydrocarbons (wt.%) and certain geochemical parameters for the Qinghai Lake sediments.

Carbon numbers	QH2-1	QH2-2	QH2-3	QH2-4	QH2-5	QH2-6	Average
C12	0	0.08	0	0	0	0	0.02
C13	0.14	0.88	0.21	0.34	0.14	0.26	0.31
C14	1.76	2.64	0.96	1.74	1.26	1.80	1.56
C15	5.12	4.60	3.00	3.65	2.94	3.56	3.54
C16	6.91	5.99	5.41	5.68	4.56	5.15	5.22
C17	6.30	5.52	6.11	6.48	4.82	5.41	5.36
C18	3.89	3.15	3.83	4.29	3.15	3.07	3.33
C19	2.78	2.45	2.98	3.27	2.21	2.80	2.53
C20	1.65	1.45	1.92	1.99	1.38	1.81	1.56
C21	2.27	2.23	2.51	2.62	1.98	2.46	2.16
C22	2.04	2.01	2.32	2.57	1.93	2.28	2.02
C23	4.91	5.42	5.43	6.41	4.88	4.89	5.32
C24	2.11	2.54	2.64	2.83	2.50	2.35	2.49
C25	6.05	7.98	7.30	7.94	8.00	6.98	7.37
C26	2.10	2.68	2.52	2.81	3.00	2.42	2.59
C27	9.28	10.88	10.62	10.13	12.36	10.47	10.62
C28	2.34	2.68	2.52	2.50	2.83	2.36	2.54
C29	17.07	15.00	16.66	13.18	18.84	17.45	16.37
C30	1.56	1.79	1.61	1.79	1.93	1.72	1.73
C31	14.61	12.40	12.68	10.52	14.68	14.39	13.21
C32	0.42	0.53	0.50	0.76	0.52	0.54	0.54
C33	0.30	0.40	0.10	0.13	0.13	0.16	0.20
C34	0	0.08	0	0	0	0	0.02
C35	0	0.03	0	0	0	0	0.01
Max peak	C29	C29	C29	C29	C29	C29	
Pr	3.94	4.04	4.68	4.55	3.65	4.24	4.18
Ph	2.46	2.57	3.49	3.83	2.31	3.44	3.02
Pr/Ph	1.60	1.57	1.34	1.19	1.58	1.23	1.42
CPI	6.47	5.29	5.73	4.63	5.76	6.15	5.67
OEP	8.11	6.34	7.47	5.81	7.35	7.94	7.17
Pr/nC17	0.63	0.73	0.77	0.70	0.76	0.78	0.73
Ph/nC18	0.63	0.81	0.91	0.89	0.73	1.12	0.85
C21−/C22+	0.49	0.45	0.41	0.49	0.31	0.40	0.43
C(21+22)/C(28+29)	0.22	0.24	0.25	0.33	0.18	0.24	0.24

Pr: pristane; Ph: phytane; CPI: carbon preference index; OEP: odd-even predominance
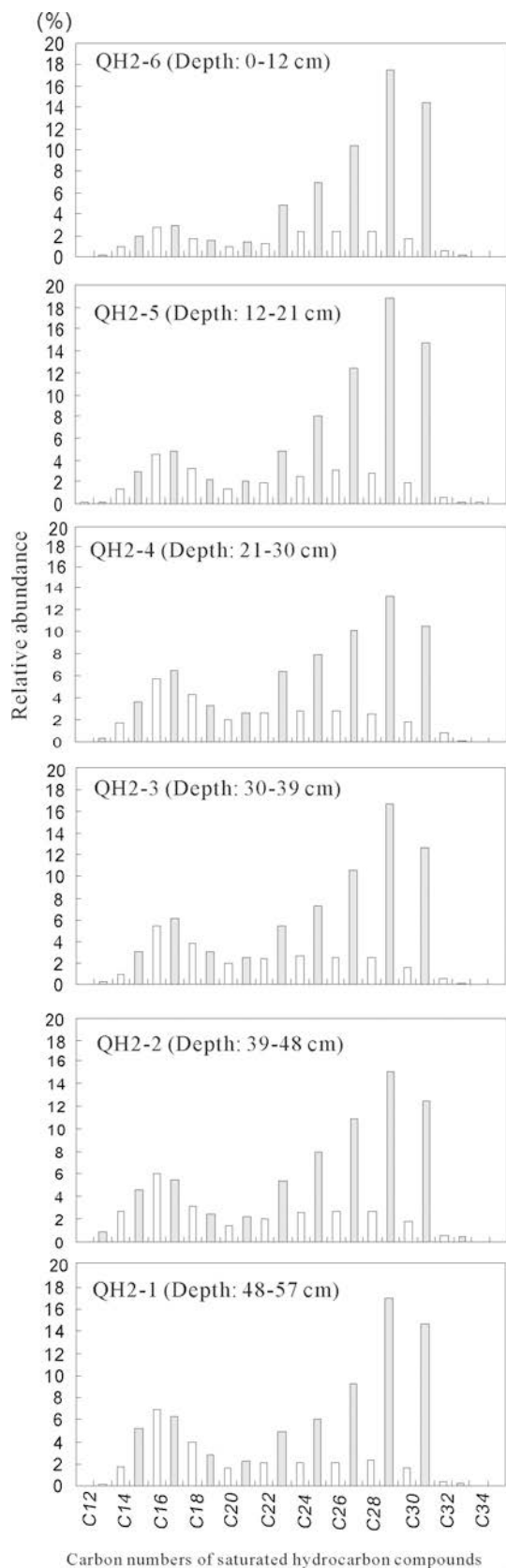
geochemical parameters reflect overall changes as a result of abiotic and biotic actions as discussed below.

DISCUSSION

Source of organic matter in the Qinghai Lake sediments

Organic compounds of saturated hydrocarbons with large carbon numbers ($>C_{22}$) and large OEP values (up to 10) are generally accepted as being derived from plants with greater proportions of wax (Eglinton and Calvin, 1967; Kolattukudy *et al.*, 1976; Simoneit and Mazurek, 1982; Hu and Disnar, 1995; Huang *et al.*, 1999; Xie *et al.*, 2003). In contrast, organic compounds derived from microorganisms and algae are characterized by small to medium carbon numbers ($<C_{21}$) (Weete, 1976; Wakeham, 1990). The characteristic bimodal distribution of carbon compounds in the Qinghai Lake sediments (Figure 6) suggest that organic matter was derived from these two sources. The characteristically large OEP values and the dominant high-C peak (C29) suggest that the C23−C33 compounds were derived from terrestrial plants; whereas the compounds with smaller carbon numbers (C12−C20) were possibly derived from microorganisms and algae.

Qinghai Lake has >70 inflowing rivers in the northern sub-basin (Sciences, 1979). These rivers cover a large watershed with abundant plants around the lake. Because of the small amount of biomass in the water column overall ($\sim 10^6$ cells/mL) (Jiang *et al.*, 2008) and, as a result, a small rate and limited extent of organic-matter degradation by heterotrophic organisms, the majority of the plant-derived organic matter is probably buried in the sediments, as shown by the presence of abundant pollen in the low-density fraction of the sediments (Figure 3c). Although nutrient levels are generally low in Qinghai Lake (Sciences, 1979), previous data suggest that microorganisms are present and active in both the lake water and sediments (Dong *et al.*, 2006; Jiang *et al.*, 2008). Thus, the compounds with smaller carbon numbers (C12−C20) were probably derived from *in situ* photosynthetic activity.

Occurrence of organic matter in relation to clay minerals

Clay minerals are characterized by small grain size and large surface area (Zhao and Zhang, 1990). Because

Figure 6. Distribution patterns of carbon compounds of the saturated hydrocarbon fraction showing the relative change of the two main peaks with depth. Whereas the relative abundance of small carbon number (<C21) saturated hydrocarbons increases with depth, that of the large carbon number compounds decreases. Furthermore, the C_{max} of the small-carbon peaks shifts from C17 above a depth of 30 cm to C16 below this depth. See text for discussion. The unshaded and shaded bars refer to even- and odd-numbered carbon compounds, respectively.
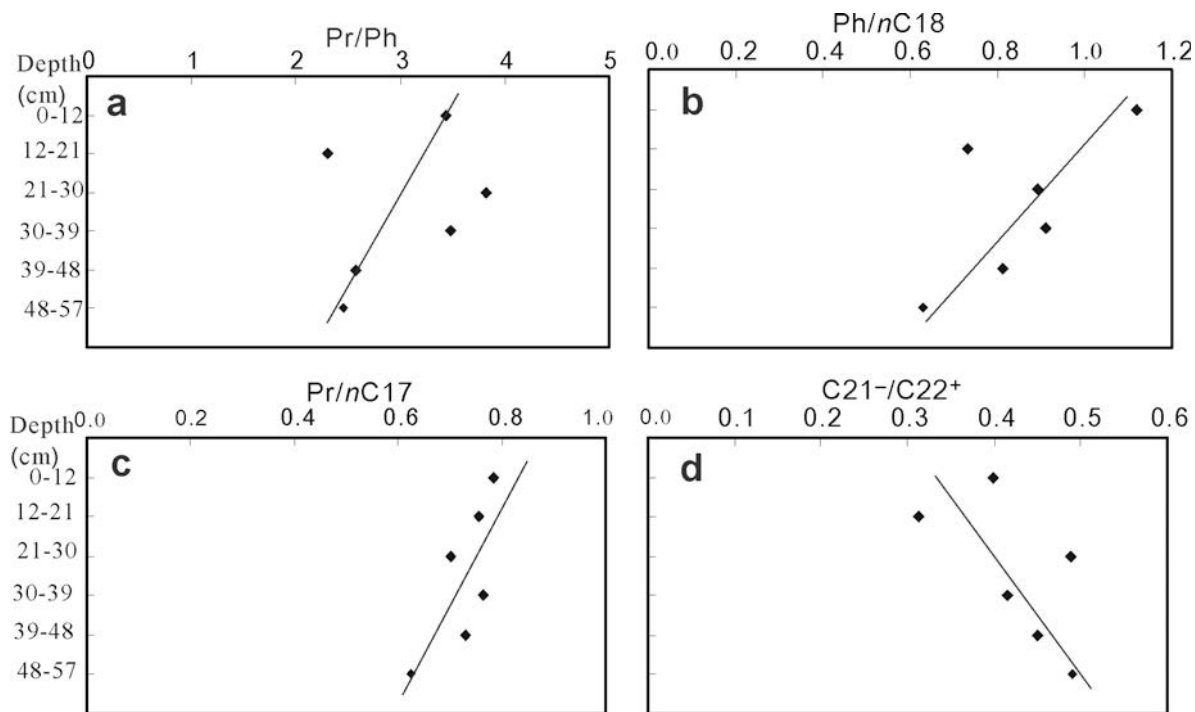
Figure 7. Change of some organic geochemical parameters with depth in the Qinghai Lake sediments. Pr: pristane; Ph: phytane.

the large surface area greatly facilitates sorption of organic matter, it is typically associated with rocks and sediments with abundant clay minerals. The present data are consistent with this general trend. For example, the average abundance of clay minerals in the mid-density fraction is 50.9%, which represents a 38.3% increase relative to that in the bulk sediments. Correspondingly, the TOC content in this fraction increased by 56% (relative to that in the bulk sediments). The following calculation illustrates this quantitative correspondence:

$$\text{Average MSA}_{\text{mid-density}}/\text{Average MSA}_{\text{high-density}} = 1.85$$

$$\text{Average TOC}_{\text{mid-density}}/\text{Average TOC}_{\text{high-density}} = 1.60$$

The positive correlation between TOC and MSA (Figure 4) further confirms that organic matter is associated with clay minerals, consistent with observations of previous studies (Mayer, 1994a, 1994b; Kennedy et al., 2002). Such a correlation is apparently true for young and old marine and lake sediments, regardless of specific clay mineralogy. The TEM observations in the present study, of a mid-density fraction from a depth of 25 cm, reveal that organic matter is closely associated with illite and chlorite packets (Figure 2), forming clay mineral-organic matter aggregates. This occurrence of organic matter was expected, based on the oxygen exposure time (OET) which was calculated as the oxygen penetration depth in sediment pore waters divided by the sedimentation rate (Hedges and Keil, 1995). According to this definition,

OET is ~200 y at a depth of 25 cm, assuming a sedimentation rate of 1.2 mm/y (Sciences, 1979). According to the conclusion of Arnarson and Keil (2007), organic matter should occur predominantly in the form of organic-mineral aggregates in sediments with OETs of years to decades. The present data are, therefore, in agreement with this conclusion.

Organic matter preservation in the Qinghai Lake sediments

Microbial activity in sediments plays a major role in determining whether organic carbon is recycled or buried (Weston and Joye, 2005). This microbe-organic matter interaction is impacted by the sediment redox state. For the Qinghai lake sediments, the water-sediment interface was oxic and became less oxic/more reducing with depth, as indicated by the decreased Pr/Ph ratio (Figure 7a), color, and mineralogical changes (framboidal pyrite and H_2S gas at depth). Under oxidizing conditions near the sediment surface, microbial abundance is greatest (Figure 5b), and presumably the microbes are active. Thus, heterotrophic microorganisms would readily oxidize the labile fraction of organic matter, accounting for the greater extent of degradation of both bulk organic matter (Figure 5a) and low-carbon compounds of saturated hydrocarbons at the water-sediment interface (the top graph of Figure 6, Figure 7d). Deeper in the sediments (>~12 cm), the less oxic/more reducing conditions would inhibit aerobic microbial activity and decrease the overall microbial

abundance. The smaller microbial abundance and degree of activity would in turn result in the reduced extent of degradation of both bulk organic matter and low-carbon compounds of saturated hydrocarbons (Figures 5a, 6).

The microbial effect on organic-matter degradation was expected to be different for labile and refractory organic compounds, depending on their occurrence of organic matter in relation to clay minerals. Under oxidizing conditions near the water-sediment interface, the low-carbon compounds of saturated hydrocarbons may occur in adsorbed form (onto external clay mineral surfaces) and in organic matter-clay mineral aggregates. The high-carbon compounds occur as discrete particles in isolation with clay minerals (such as pollens, Figure 3c). In this case, both types of compounds (low- and high-carbon compounds) are susceptible to microbial degradation. At depths, under reducing conditions, the adsorbed fraction (probably labile) may have already been degraded, and the fraction in organic matter-clay mineral aggregates may be the predominant form of the low-carbon compounds. The encapsulated low-carbon compounds within organic matter-clay mineral aggregates may be protected from enzymatic degradation (Sollins *et al.*, 1996; Baldock and Skjemstad, 2000; Six *et al.*, 2002; Curry *et al.*, 2007) and thus may account for the relative increase in abundance of the low-carbon compounds (bottom graph, Figure 6). In contrast, the high-carbon compounds (such as pollen) still occur as discrete materials and should still be susceptible to microbial degradation under reducing conditions, and any degradation products should be easily lost from the sediments (and thus not measured by the carbon compound analysis), apparently due to their open access to large pores and possibly oxygen.

CONCLUSIONS

In summary, under both oxidizing and reducing conditions, the rate and extent of microbial degradation of the low-carbon compounds should be greater than the rate for the high-carbon compounds, because the low-carbon fraction should be more labile. However, near the top of the core, the rate and extent of microbial degradation of the low-carbon compounds may be much greater than the rate and extent of biodegradation of the high-carbon compounds, because the low-carbon compounds are more labile. In comparison, at depths, the difference in the rate and extent of biodegradation of low- and high-carbon compounds may not be as great as that near the top of the core, because only the high-carbon compounds are accessible to microorganisms (and the low-carbon compounds are protected within the clay mineral-organic matter aggregates). Therefore, the differential rate and extent of biodegradation of low- and high-carbon compounds as a function of burial depth are responsible for the observed pattern of organic-compound distribution (Figure 6).

REFERENCES

An, Z.S. (2003) *Scientific Drilling at Qinghai Lake on the Northwestern Tibetan Plateau: High-Resolution Paleoenvironmental Records of Eastern Asia and Their Significance for Global Change*. Lake Qinghai Workshop, Institute of Earth Environment, Chinese Academy of Sciences, Xining, China, pp. 1−2.

Arnarson, T.S. and Keil, R.G. (2001) Organic-mineral interactions in marine sediments studied using density fractionation and X-ray photoelectron spectroscopy. *Organic Geochemistry*, **32**, 1401−1415.

Arnarson, T.S. and Keil, R.G. (2007) Changes in organic matter-mineral interactions for marine sediments with varying oxygen exposure times. *Geochimica et Cosmochimica Acta*, **71**, 3545−3556.

Bader, R.G., Hood, D.W., and Smith, J.B. (1970) Recovery of dissolved organic matter in seawater and organic sorption by particulate material. *Geochimica et Cosmochimica Acta*, **19**, 236−243.

Baldock, J.A. and Skjemstad, J.O. (2000) Role of the soil matrix and minerals in protecting natural organic materials against biological attack. *Organic Geochemistry*, **31**, 697−710.

Bergamashi, B.A., Tsamakis, E., Keil, R.A., Eglington, T.I., Montlucon, D.B., and Hedges, J.I. (1997) The effect of grain size and surface area on organic matter, lignin and carbohydrate concentration, and molecular compositions in Peru Margin sediments. *Geochimica et Cosmochimica Acta*, **61**, 1247−1260.

Bishop, A.N. and Phillip, R.P. (1994) Potential for amorphous kerogen formation via adsorption of organic material at mineral surfaces. *Energy and Fuels*, **8**, 1494−1497.

Bishop, A.N., Kearsley, A.T., and Patience, R.L. (1992) Analysis of sedimentary organic materials by scanning electron microscopy: the application of back scattered electron imagery and light element X-ray microanalysis. *Organic Geochemistry*, **18**, 431−446.

Bock, M.J. and Mayer, L.A. (2000) Mesodensity organo-clay associations in a near shore sediment. *Marine Geology*, **163**, 65−75.

Christidis, G. and Eberl, D.D. (2003) Determination of layer-charge characteristics of smectites. *Clays and Clay Minerals*, **51**, 644−655.

Collins, M.J., Bishop, A.N., and Farrimond, P. (1995) Sorption by mineral surfaces: Rebirth of the classical condensation pathway for kerogen formation? *Geochimica et Cosmochimica Acta*, **59**, 2387−2391.

Curry, K.J., Bennett, R.H., Mayer, L.M., Curry A., Abril, M., Biesiot, P.M., and Hulbert, M.H. (2007) Direct visualization

of clay microfabric signatures driving organic matter preservation in fine-grained sediment. *Geochimica et Cosmochimica Acta*, **71**, 1709−1720.

Didyk, B.M., Simoneit, B.M., Brassell, S.C., and Eglinton, G. (1987) Organic geochemical indicators of palaeoenvironmental conditions of sedimentation. *Nature (London)*, **272**, 216−222.

Dong, H., Zhang, G., Jiang, H., Yu, B. Chapman, L.R., Lucas, C.R., and Fields, M.W. (2006) Microbial diversity in sediments of saline Qinghai Lake, China: Linking geochemical controls to microbial ecology. *Microbial Ecology*, **51**, 65−82.

Eberl, D.D. (2003) *User guide to RockJock−A program for determining quantitative mineralogy from X-ray542 diffraction data.* U.S. Geological Survey Open File Report OF 03-78. 40 pp.

Eglinton, G. and Calvin, M. (1967) Chemical fossils. *Scientific American*, **216**, 32−43.

Golchin, A., Oades, J.M., Skjemstad, J.O., and Clarke, P. (1994) Soil structure and carbon cycling. *Australian Journal of Soil Research*, **32**, 1043−1068.

Gordon, A.S. and Millero, F.J. (1985) Adsorption mediated decrease in the biodegradation rate of organic compounds. *Microbial Ecology*, **11**, 289−298.

Hedges, J.I. and Keil, R.G. (1995) Sedimentary organic matter preservation: An assessment and speculative synthesis. *Marine Chemistry*, **49**, 81−115.

Hedges, J.I. and Keil, R.G. (1999) Organic geochemical perspective on estuarine processes: sorption reactions and consequences. *Marine Chemistry*, **65**, 55−65.

Hedges, J.I. and Oades, J.M. (1997) Comparative organic geochemistries of soils and marine sediments. *Organic Geochemistry*, **27**, 319−361.

Heinrichs, S.M. and Sugai, S.F. (1993) Adsorption of amino acids and glucose by sediments of Resurrection Bay (Alaska): Functional group effects. *Geochimica et Cosmochimica Acta*, **57**, 823−835.

Henderson, A.C.G., Holmes, J.A., Zhang, J., Leng, M.J., and Carvalho, L.R. (2003) A carbon- and oxygen-isotope record of recent environmental change from Qinghai Lake, NE Tibetan Plateau. *Chinese Science Bulletin*, **48**, 1463−1467.

Hu, M.A. and Disnar, J.R. (1995) Organic geochemical indicators of biological sulphate reduction in early diagenetic Zn-Pb mineralization: the Bois-Madame deposit (Gard, France). *Applied Geochemistry*, **10**, 419−435.

Huang, Y., Street-Perrott, F.A., Perrott, F.A., Metzger, P., and Eglinton, G. (1999) Glacial-interglacial environmental changes inferred from the molecular and compound-specific $\delta^{13}C$ analyses of sediments from Sacred Lake, Mt Kenya. *Geochimica et Cosmochimica Acta*, **63**, 1383−1404.

Hughes, W.B., Holba, A.G., and Dzou, L.I.P. (1995) The ratios of dibenzothiophene to phenanthrene and pristane to phytane as indicators of depositional environment and lithology of petroleum source rocks. *Geochimica et Cosmochimica*, **59**, 3581−3598.

Jiang, H., Dong, H., Yu, B., Ye, Q., Shen, J., Rowe, H., and Zhang, C.L. (2008) Dominance of putative marine benthic archaea in Qinghai lake, Northwestern China. *Environmental Microbiology*, **10**, 2355−2367.

Keil, R.G. and Hedges, J.I. (1993) Sorption of organic matter to mineral surfaces and the preservation of organic material in coastal marine sediments. *Chemical Geology*, **107**, 385−388.

Kennedy, M.J., Pevear, D.R., and Hill, R.H. (2002) Mineral surface control of organic carbon in black shale. *Science*, **295**, 657−660.

Kolattukudy, P.E., Croteau, R., and Buckner, J.S. (1976) Biochemistry of plant waxes. Pp. 289−347 in: *Chemistry and Biochemistry of Natural Waxes* (P.E. Kolattukudy,

editor). Elsevier, Amsterdam.

Li, R. (1993) *Study on Organic Matter and Oil Production of the Sedimentary Rocks from Evaporate Environments.* Ocean Press, Beijing (in Chinese).

Mayer, L.M. (1994a) Surface area control of organic carbon accumulation in continental shelf sediments. *Geochimica et Cosmochimica Acta*, **58**, 1271−1284.

Mayer, L.M. (1994b) Relationship between mineral surfaces and organic carbon concentration in soils and sediments. *Chemical Geology*, **114**, 347−363.

Mayer, L.M. (1999) Extent of coverage of mineral surfaces by organic matter in marine sediments. *Geochimica et Cosmochimica Acta*, **63**, 207−215.

Peacor, D.R., Coveney, R.M., and Zhao, G. (2000) Authigenic illite and organic matter: the principal hosts of vanadium in the Mecca Quarry shale at Velpen, Indiana. *Clays and Clay Minerals*, **48**, 311−316.

Ransom, B., Bennett, R.H., Baerwald, R., and Shea, K. (1997) TEM study of in situ organic matter on continental margins: Occurrence and the monolayer hypothesis. *Marine Geology*, **138**, 1−9.

Ransom, B., Dongseon, K., Kastner, M., and Wainwright, S. (1998) Organic matter preservation on continental slopes: Importance of mineralogy and surface area. *Geochimica et Cosmachimica Acta*, **62**, 1329−1345.

Salmon, V., Derenne, S., Lallier-Verges, E., Largeau, C., and Beaudoin, B. (2000) Protection of organic matter by mineral matrix in a Cenomanian black shale. *Organic Geochemistry*, **31**, 463−474.

Sciences (1979) *Comprehensive Survey Report of Qinghai Lake.* Scientific Publishing House, Beijing (in Chinese).

Shen, J., Liu, X., Wang, S., and Matsumoto, R. (2005) Palaeoclimatic changes in the Qinghai Lake area during the last 18,000 years. *Quaternary International*, **136**, 131−140.

Simoneit, B.R.T. and Mazurek, M.A. (1982) Organic matter of the troposphere − II. Natural background of biogenic lipid matter in aerosols over the rural western United States. *Atmospheric Environment*, **16**, 2139−2159.

Six, J., Conant, R.T., Paul, E.A., and Paustian, K. (2002) Stabilization mechanisms of soil organic matter: implications for C-saturation of soils. *Plant Soil*, **241**, 155−176.

Sollins, P., Hofmann, P., and Caldwell, B.A. (1996) Stabilization and destabilization of soil organic matter: mechanisms and controls. *Geoderma*, **74**, 65−105.

Środoń, J., Drits, V.A., McCarty, D.K., Hsieh, J.C.C., and Eberl, D.D. (2001) Quantitative X-ray analysis of clay bearing rocks from random preparations. *Clays and Clay Minerals*, **49**, 514−528.

Sun, Z., Yang, F., and Zhang, Z. (1997) *Condition of Sedimentation and Emergence of Petroleum in Cenozoic Saline Lake in China.* Petroleum Industry Press, Beijing (in Chinese).

Turchenek, L.W. and Oades, J.M. (1976) Organo-mineral particles in soils [A]. Pp. 137−144 in: *Modification of Soil Structure* (W.W. Emerson, R.D. Bond and A.R. Dexter, editors). John Wiley & Sons, New York.

Wakeham, S.G. (1990) Algal and bacterial hydrocarbons in particulate matter and interfacial sediment of the Cariaco Trench. *Geochimica et Cosmochimica Acta*, **54**, 1325−1336.

Wang, T. (1990) *Study on Biomarker Geochemistry.* China University of Geosciences Publishing House, Wuhan, China (in Chinese).

Weete, J.D. (1976) Algal and fungal waxes. Pp. 349−418 in: *Chemistry and Biochemistry of Natural Waxes* (P.E. Kolattukudy, editor). Elsevier, Amsterdam.

Weston, N.B. and Joye, S.B. (2005) Temperature-driven decoupling of key phases of organic matter degradation in marine sediments. *Proceedings of the National Academy of*

Sciences of the United States of America, **102**, 17036−17040.

Xie, S., Lai, X., Yi, Y., Gu, Y., Liu, Y., Wang, X., Liu, G., and Liang, B. (2003) Molecular fossils in a Pleistocene river terrace in southern China related to paleoclimate variation. *Organic Geochemistry*, **34**, 789−797.

Zhao X. and Zhang Y. (1990) *Clay Minerals and Analytical Methods.* Ocean Press, Beijing, 43−44 (in Chinese).